Supplemental Table 1: RNA-seq datasets with corresponding orthogonal datasets used for benchmarking

RNA- seq data						**matching orthogonal data**	
SRA accession	**sample_name**	**strandedness**	**layout**	**organism**	**length**	**SRA accession**	**sequencing method**
SRR1573494	HEK293_siControl_R1	reverse	paired	Hsap	100	SRR2922409	A-seq2
SRR1573495	HEK293_siControl_R2	reverse	paired	Hsap	100	SRR2922448	A-seq2
SRR1573496	HEK293_siHNRNPC_R1	reverse	paired	Hsap	100	SRR2922419	A-seq2
SRR1573497	HEK293_siHNRNPC_R2	reverse	paired	Hsap	100	SRR2922449	A-seq2
SRR6795718	Mayr_CD5B_R3	reverse	paired	Hsap	51	SRR6795684	3'-seq
SRR6795719	Mayr_CD5B_R4	reverse	paired	Hsap	51	SRR6795685	3'-seq
SRR6795720	Mayr_NB_R1	reverse	paired	Hsap	51	SRR1005606	3'-seq
SRR6795721	Mayr_NB_R2	reverse	paired	Hsap	51	SRR1005607	3'-seq
SRR6795723	Mayr_NB_R3	reverse	paired	Hsap	51	SRR6795688	3'-seq
SRR6795724	Mayr_NB_R4	reverse	paired	Hsap	51	SRR6795689	3'-seq
SRR6795726	Mayr_M_R2	reverse	paired	Hsap	51	SRR6795691	3'-seq
SRR6795713	Mayr_GC_R2	reverse	paired	Hsap	51	SRR6795693	3'-seq
SRR6795715	Mayr_GC_R1	reverse	paired	Hsap	51	SRR6795692	3'-seq
SRR11918577	P19_siControl_R1	unstranded	single	Mmus	75	SRR11918617	MACEseq
SRR11918578	P19_siControl_R2	unstranded	single	Mmus	75	SRR11918618	MACEseq
SRR11918579	P19_siSrsf3_R1	unstranded	single	Mmus	75	SRR11918619	MACEseq
SRR11918580	P19_siSrsf3_R2	unstranded	single	Mmus	75	SRR11918620	MACEseq
SRR11918581	P19_siSrsf7_R1	unstranded	single	Mmus	75	SRR11918621	MACEseq
SRR11918582	P19_siSrsf7_R2	unstranded	single	Mmus	75	SRR11918622	MACEseq
SRR1811005	MmusCortex_adult_R1	forward	paired	Mmus	37	GSM1614167	PAPERCLIP
SRR3067958	MmusCortex_adult_R2	forward	paired	Mmus	35	GSM1614167	PAPERCLIP
SRR3067957	MmusCortex_embryonic_R1	forward	paired	Mmus	37	GSM1614169	PAPERCLIP
SRR3067959	MmusCortex_embryonic_R2	forward	paired	Mmus	35	GSM1614169	PAPERCLIP
SRR22955576	GTEXsim_cerebellum_R1	forward	paired	Hsap	100	simulatedPAS	simulated
SRR22955574	GTEXsim_cerebellum_R2	forward	paired	Hsap	100	simulatedPAS	simulated
SRR22955639	GTEXsim_cerebellum_R3	forward	paired	Hsap	100	simulatedPAS	simulated
SRR22955510	GTEXsim_cerebellum_R4	forward	paired	Hsap	100	simulatedPAS	simulated
SRR22955630	GTEXsim_cerebellum_R5	forward	paired	Hsap	100	simulatedPAS	simulated
SRR22955420	GTEXsim_cerebellum_R6	forward	paired	Hsap	100	simulatedPAS	simulated
SRR22955571	GTEXsim_cerebellum_R7	forward	paired	Hsap	100	simulatedPAS	simulated
SRR22955570	GTEXsim_cerebellum_R8	forward	paired	Hsap	100	simulatedPAS	simulated
SRR22955441	GTEXsim_cerebellum_R9	forward	paired	Hsap	100	simulatedPAS	simulated
SRR22955647	GTEXsim_cerebellum_R10	forward	paired	Hsap	100	simulatedPAS	simulated
SRR22955539	GTEXsim_muscle_R1	forward	paired	Hsap	100	simulatedPAS	simulated

SRR22955532	GTEXsim_muscle_R2	forward	paired	Hsap	100	simulatedPAS	simulated
SRR22955403	GTEXsim_muscle_R3	forward	paired	Hsap	100	simulatedPAS	simulated
SRR22955603	GTEXsim_muscle_R4	forward	paired	Hsap	100	simulatedPAS	simulated
SRR22955459	GTEXsim_muscle_R5	forward	paired	Hsap	100	simulatedPAS	simulated
SRR22955398	GTEXsim_muscle_R6	forward	paired	Hsap	100	simulatedPAS	simulated
SRR22955458	GTEXsim_muscle_R7	forward	paired	Hsap	100	simulatedPAS	simulated
SRR22955611	GTEXsim_muscle_R8	forward	paired	Hsap	100	simulatedPAS	simulated
SRR22955449	GTEXsim_muscle_R9	forward	paired	Hsap	100	simulatedPAS	simulated
SRR22955444	GTEXsim_muscle_R10	forward	paired	Hsap	100	simulatedPAS	simulated

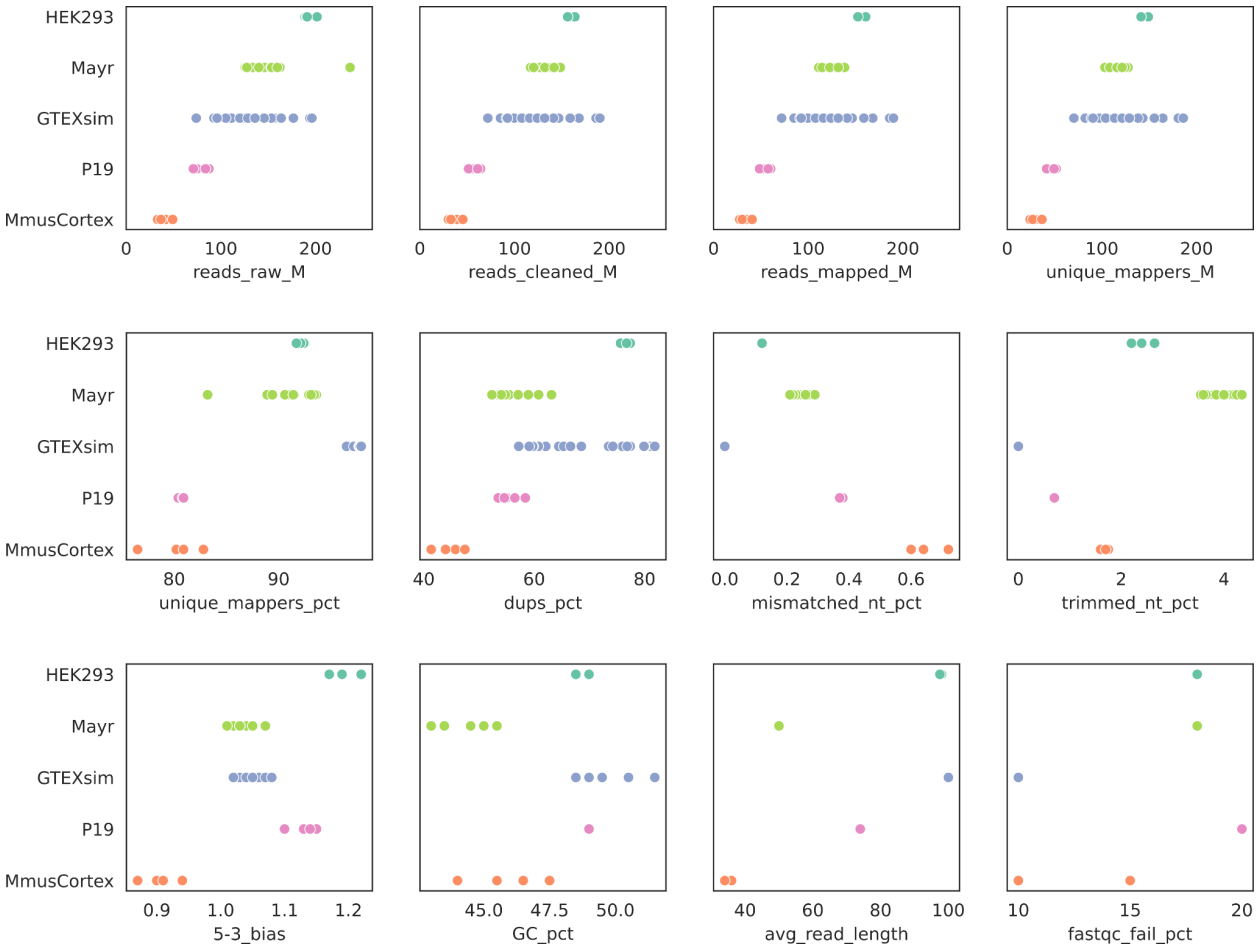

Supplemental Figure 1: Dataset characteristics. Quality characteristics of the RNA-seq datasets used for benchmarking. reads_raw_M: number of raw reads (Mio); reads_cleaned_M: number of reads after adapter trimming and minimum length selection (Mio); reads_mapped_M: number of reads successfully mapped to the genome (Mio); unique_mappers_M: number of reads mapped to a unique position in the genome (Mio); unique_mappers_pct: fraction of total reads mapped to a unique position in the genome; dups_pct: percentage of duplicate reads; mismatched_nt_pct: average percentage of mismatched nucleotides within a read; trimmed_nt_pct: average percentage of nucleotides trimmed from a read; 5-3_bias: ratio between 5' and 3' bias, where those biases are the ratio between mean coverage at the 5' region and 3' region, respectively, and the whole transcript; GC_pct: average percentage of GC nucleotides per read; avg_read_length: average read length in nucleotides; fast_qc_fail_pct: Percentage of tests failed in FastQC report of nf-core/rnaseq .

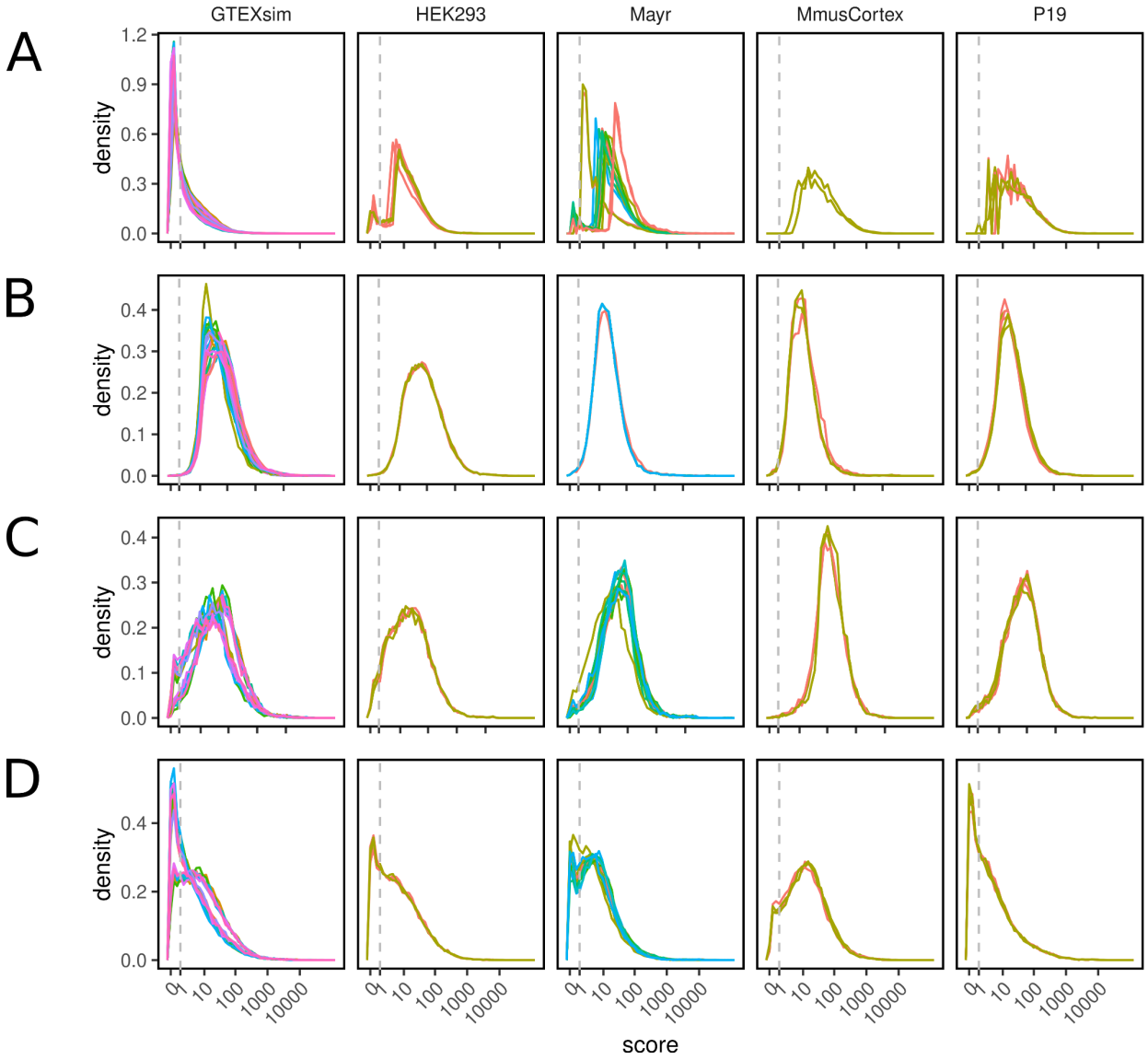

Supplemental Figure 2. TPM distributions for (A) ground truth datasets (GT), (B) APAtrap, (C) PAQR and (D) QAPA predictions (from top to bottom). The TPM scores are displayed in log-space. Sample replicates colored for better differentiation. Only all annotations (for GT) and preferred annotation (for predictions) shown.

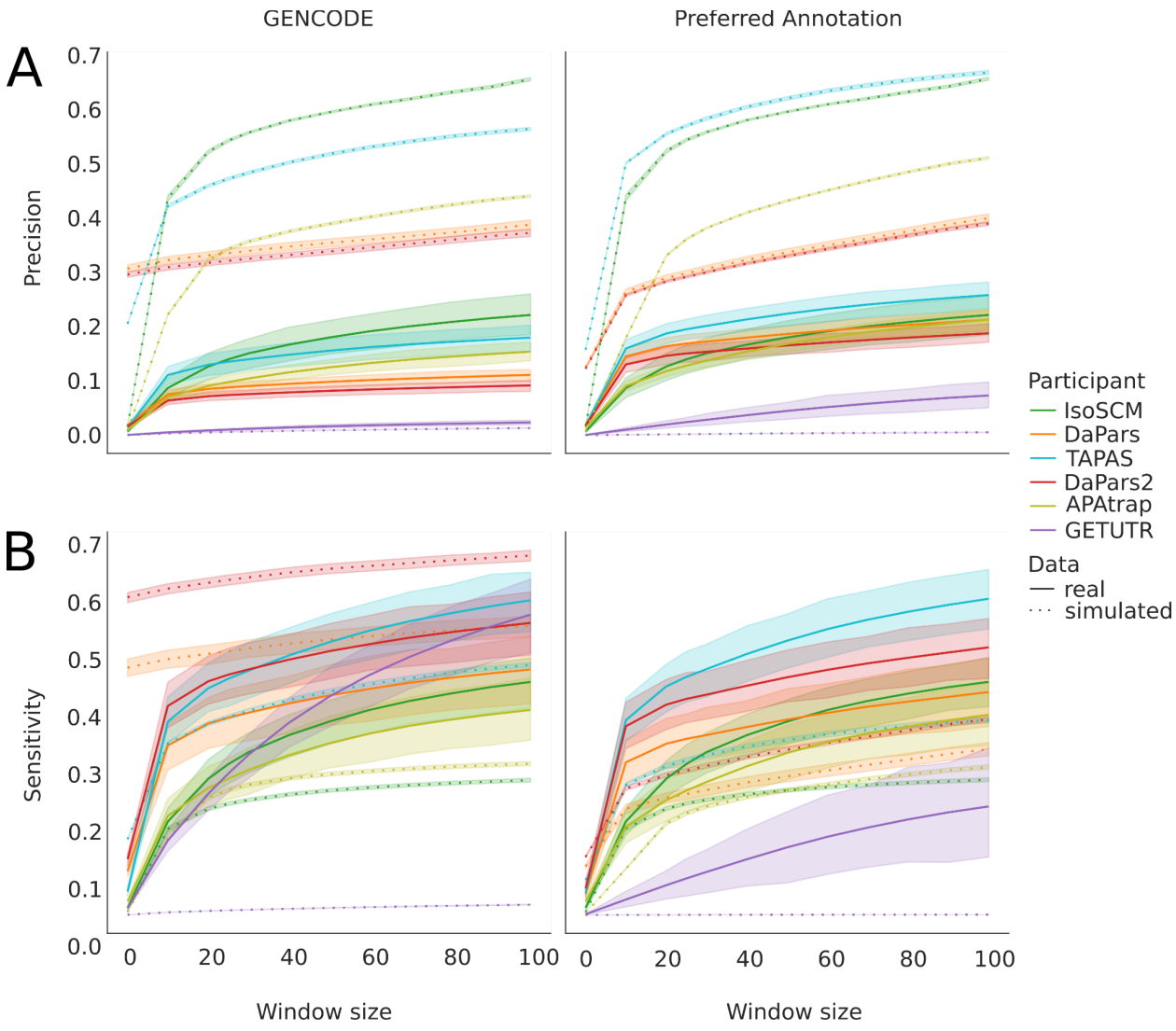

Supplemental Figure 3: Dependence of method performance in identification event on window size. Windows between 0 and 100 nt in steps of 10nt have been tested. Performance on all samples from all datasets has been combined. Shaded areas around the lines depict the 95% confidence interval. A) Precision; left column: GENCODE annotation, right column: preferred annotation. B) Sensitivity; columns as above.

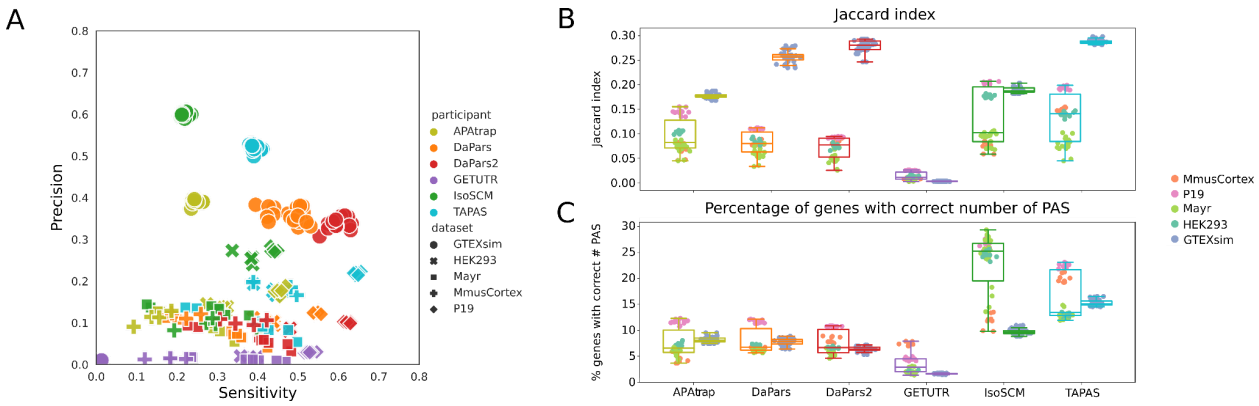

Supplemental Figure 4: Results of the PAS identification event (like Figure 2 but GENCODE instead of preferred annotation)

Box plots of Jaccard indices indicating the overlap of predicted and ground truth sites, with predicted sites being extended symmetrically by 50 nucleotides. The tools used to predict the sites are shown on the x-axis, each with two associated box plots, one for the real data (left) and another for simulated data (right). Each point is labeled according to the code given in the legend.

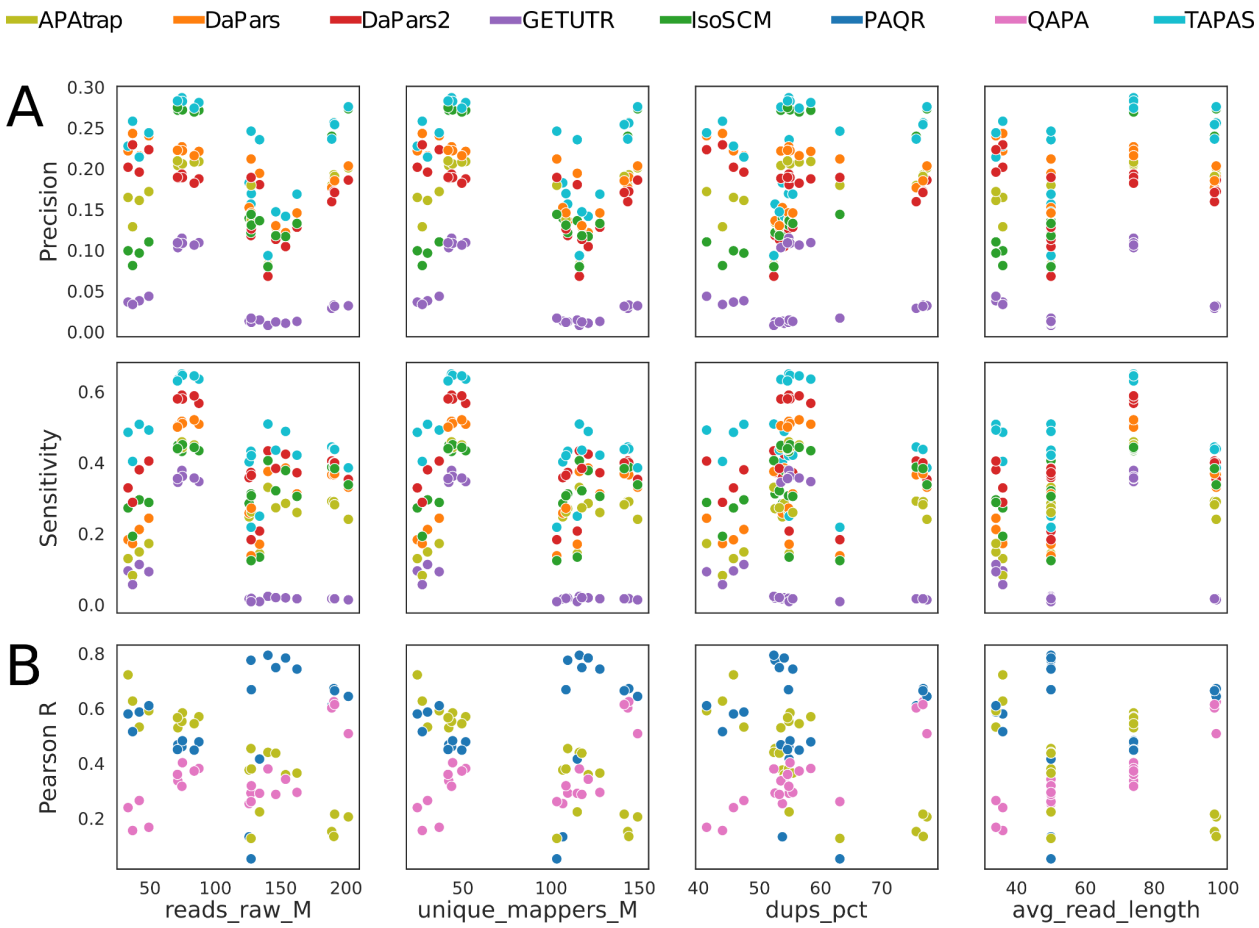

Supplemental Figure 5: Methods' performance in relation to selected dataset characteristics of real data. A) Precision and Sensitivity from the identification event. B) Pearson R from the absolute Quantification event. Each dot represents one sample.

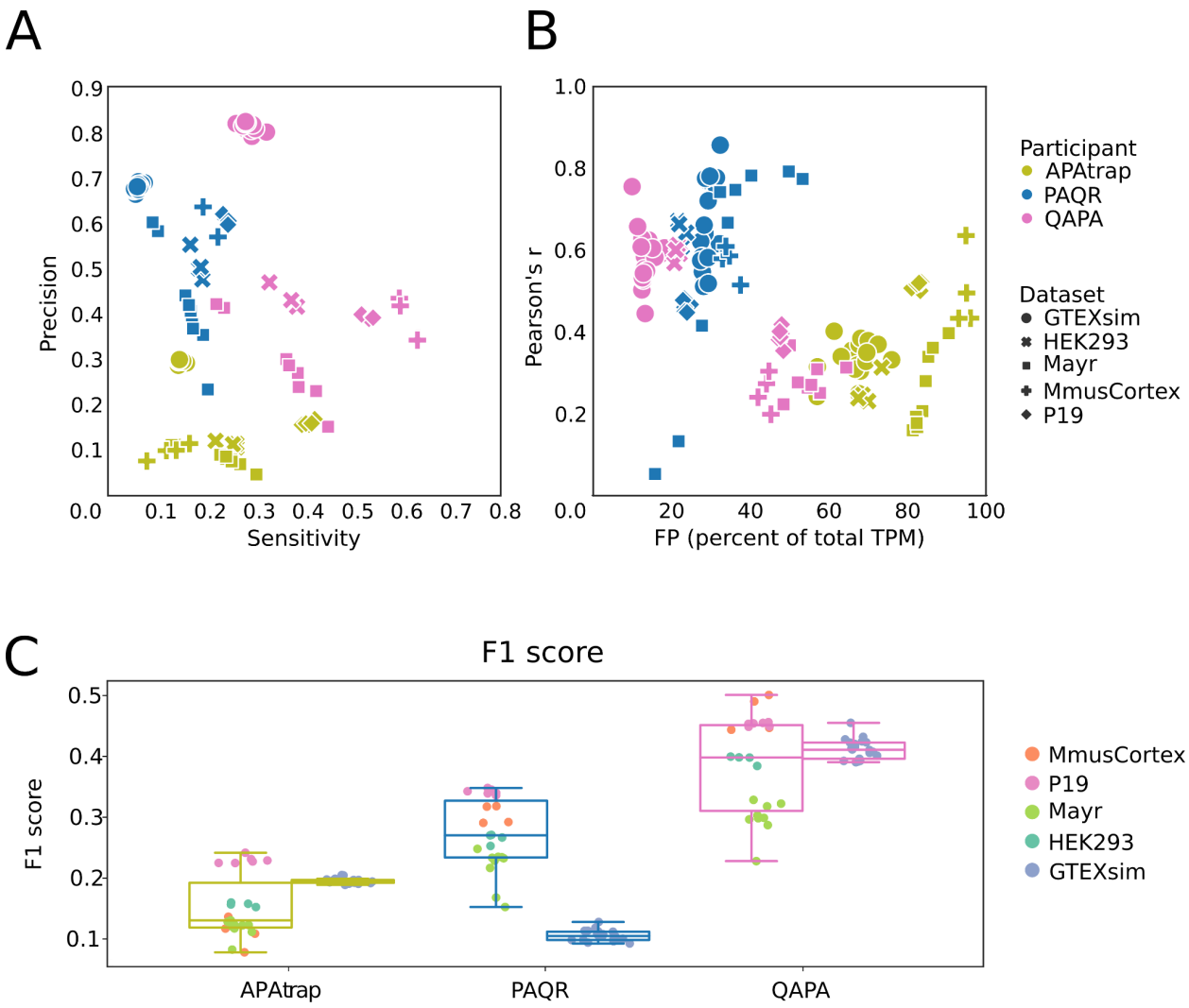

Supplemental Figure 6: Results of PAS isoform quantification (like Figure 3 but GENCODE instead of preferred annotation).

A) Scatter plot of Precision vs. Sensitivity. Each sample and tool combination is represented as a symbol, with shape and color defined in the legend. B) Pearson correlation of PD and GT site expression. The correlation coefficient for each sample is plotted against the percentage of total TPM that an algorithm attributes to PAS that are not expressed in the ground truth (false positives). C) Box plots of F1 scores. Box plots are drawn separately for real (left, see color scheme in the legend) and simulation (right) samples.

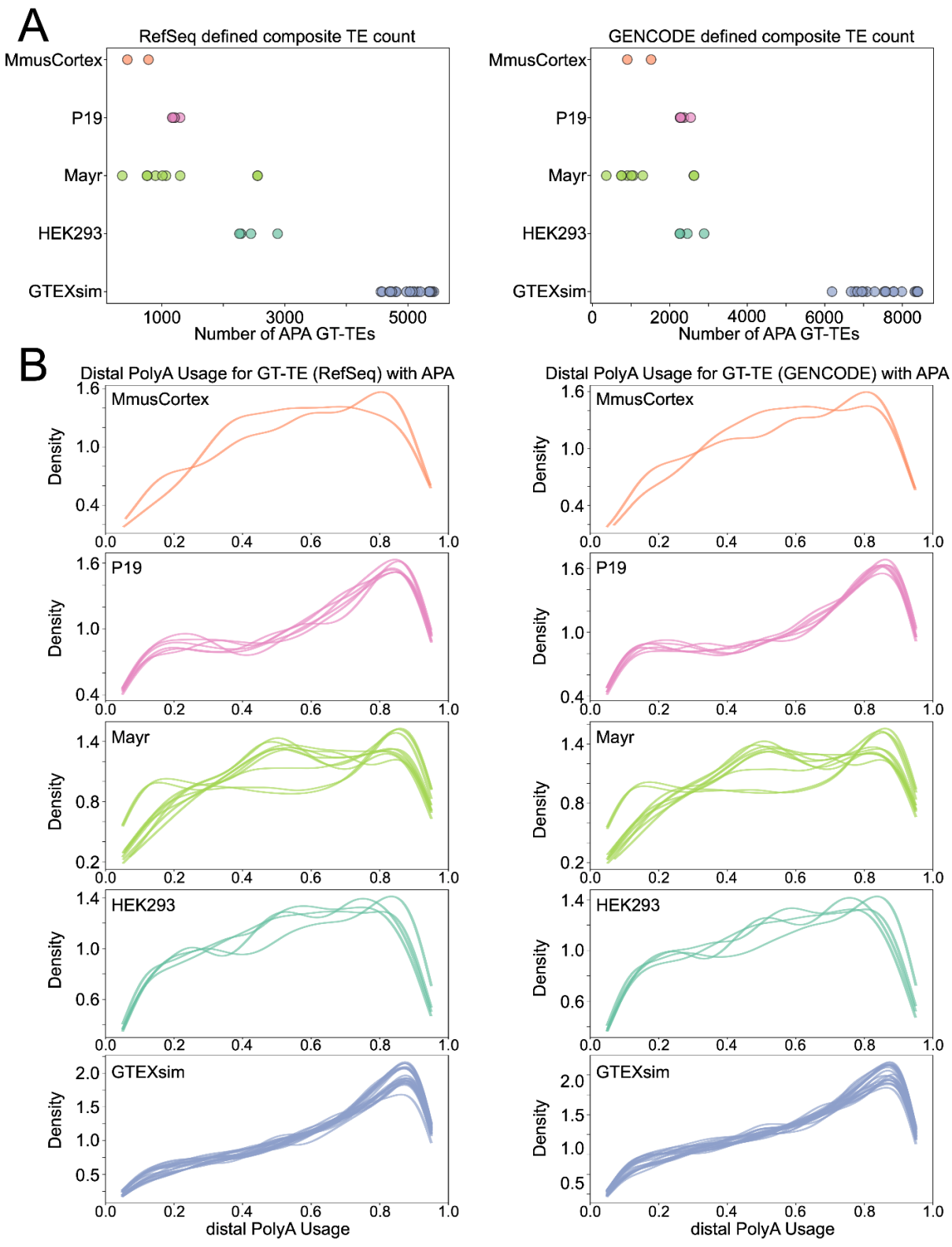
A
RefSeq defined composite TE count
GENCODE defined composite TE count
MmusCortex
P19
Mayr
HEK293
GTEXsim
1000
3000
5000
0
2000
4000
6000
8000
Number of APA GT-TEs
B
Distal PolyA Usage for GT-TE (RefSeq) with APA
Distal PolyA Usage for GT-TE (GENCODE) with APA
Density
distal PolyA Usage
0.0
0.2
0.4
0.6
0.8
1.0

Supplemental Figure 7. Characteristics of high confidence, ground-truth (GT) terminal exon (TE) with alternative polyadenylation (APA) for relative quantification benchmarking. (A) Number of composite GT-TEs with APA defined as in Figure 4 using either RefSeq (left) or GENCODE (right) annotations. Each dot represents a ground truth experimental/simulation sample. (B) Distribution of distal polyA Usage (dPAU) for GT-TEs with APA for each GT experiment separated by experimental group based on composite TEs from RefSeq (left) or GENCODE (right).

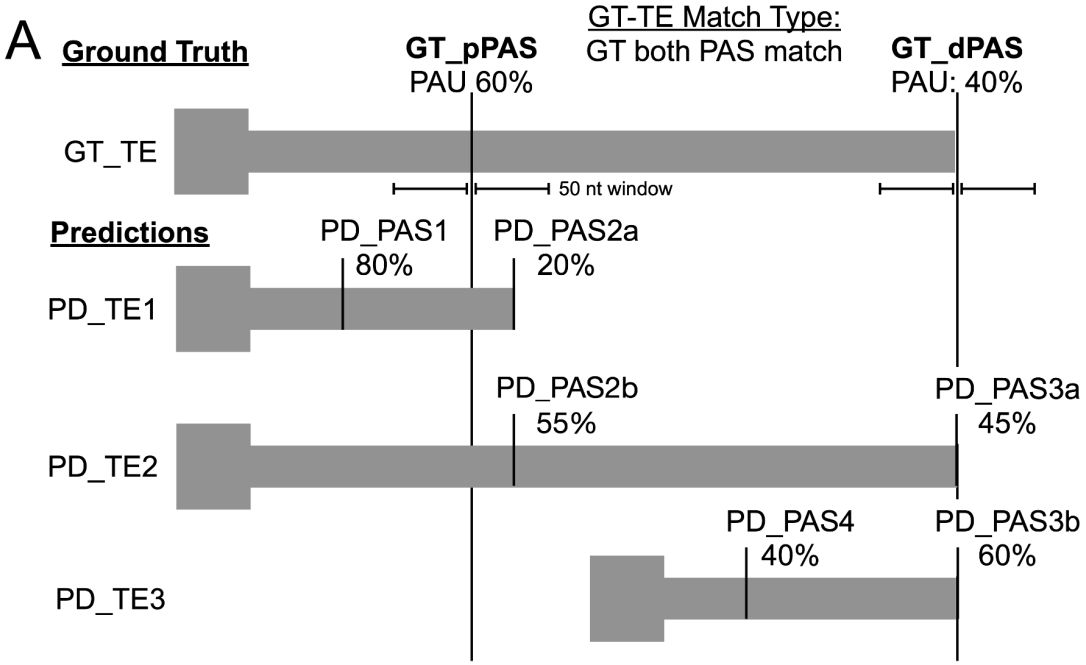

B

	GT-allPAS match?	GT-pPAS match?	GT-dPAS match?	best-PD correlation?	all-PD correlation?
PD_PAS1					
PD_PAS2a	Yes	Yes			Yes (GT_pPAS)
PD_PAS2b	Yes	Yes		Yes (GT_pPAS)	Yes (GT_pPAS)
PD_PAS3a	Yes		Yes	Yes (GT_dPAS)	Yes (GT_dPAS)
PD_PAS3b	Yes		Yes		Yes (GT_pPAS)
PD_PAS4					

Supplemental Figure 8. Multi-match examples for certain algorithm PD to GT-PAS matches. (A) Top shows an example of a theoretical high-confidence, alternative polyadenylation containing ground-truth (GT) terminal exon (TE) and proximal PAS (GT_pPAS) and distal PAS (GT_dPAS) with polyadenylation usage (PAU) calculated by the filtering algorithm described in Methods. Bottom shows an example of an algorithm like DaPars which outputs a number TEs (PD-TEs) based on each transcript with predicted PD-PAS, some of which overlap and can have different relative quantification values (e.g. PD_PAS2a versus PD_PAS2b). (B) Table showing the different match types for each PD-PAS. “best-PD” column shows only the best match between unique GT-PAS and PD-PAS which minimizes the absolute difference between the two while “all-PD” column shows all PD-PAS to GT-PAS matches which can be used for downstream benchmarking.

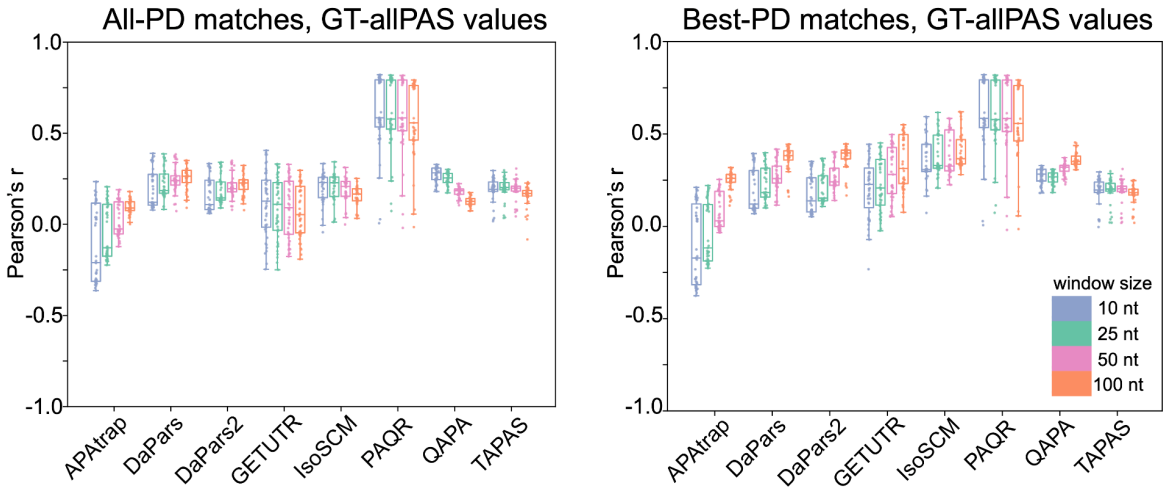

Supplemental Figure 9. Boxplots of Pearson correlation coefficients for all datasets using given window sizes and considering all PD- to GT-PAS quantification matches (left) or only the best possible PD- to GT-PAS match (right).

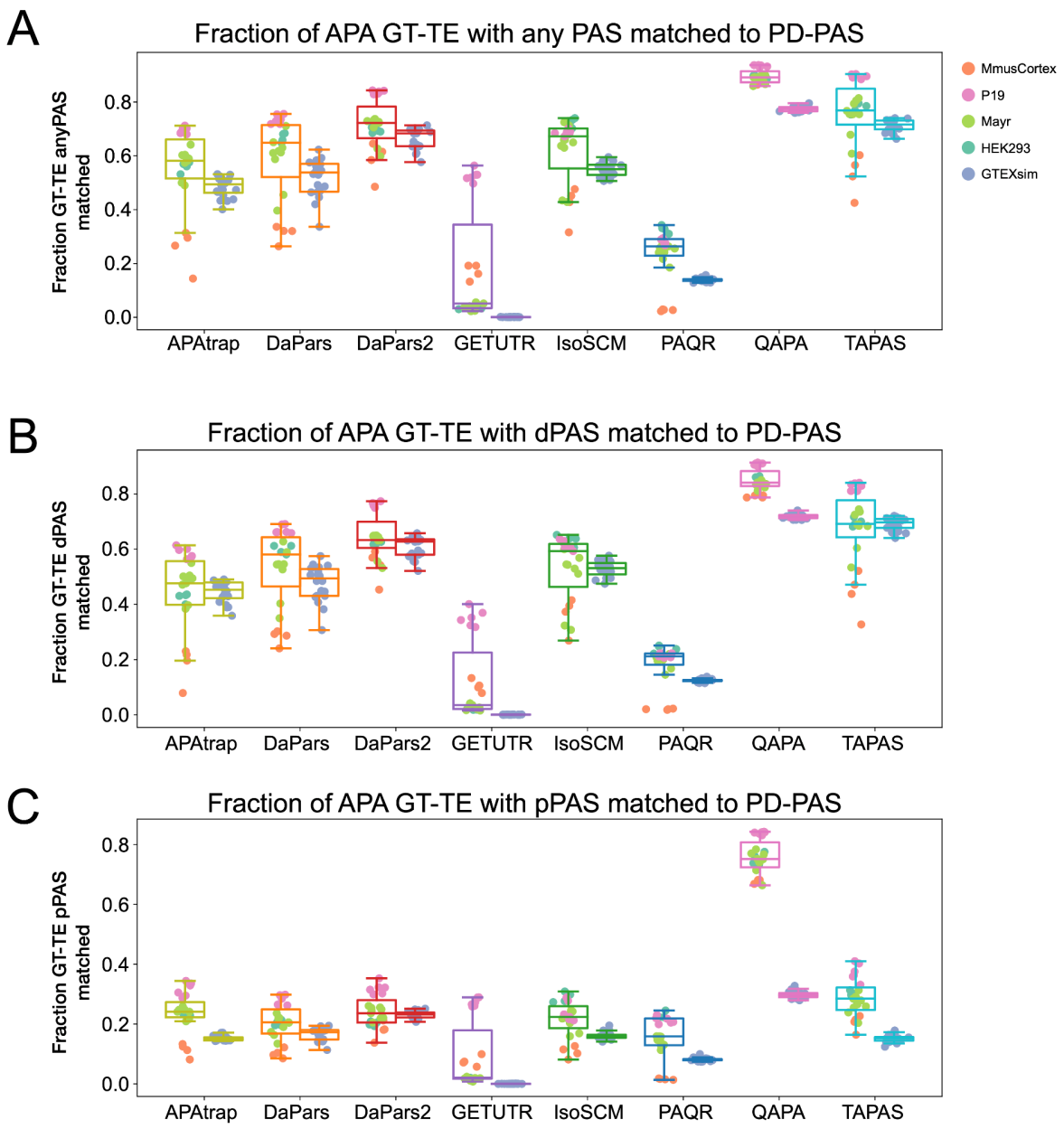

Supplemental Figure 10. (A) Fraction of unique ground truth terminal exons with alternative polyadenylation (APA GT-TE, based on RefSeq annotations) that matched to any algorithm predicted PAS (PD-PAS) using a window of 50 nucleotides. (B) Fraction of unique APA GT-TEs that had algorithm prediction PAS matched at least the distal PAS (GT-dPAS). (C) Fraction of unique terminal exons (TEs) from the ground-truth (GT) filtering that had algorithm prediction PAS matched at least the proximal PAS (GT-pPAS).

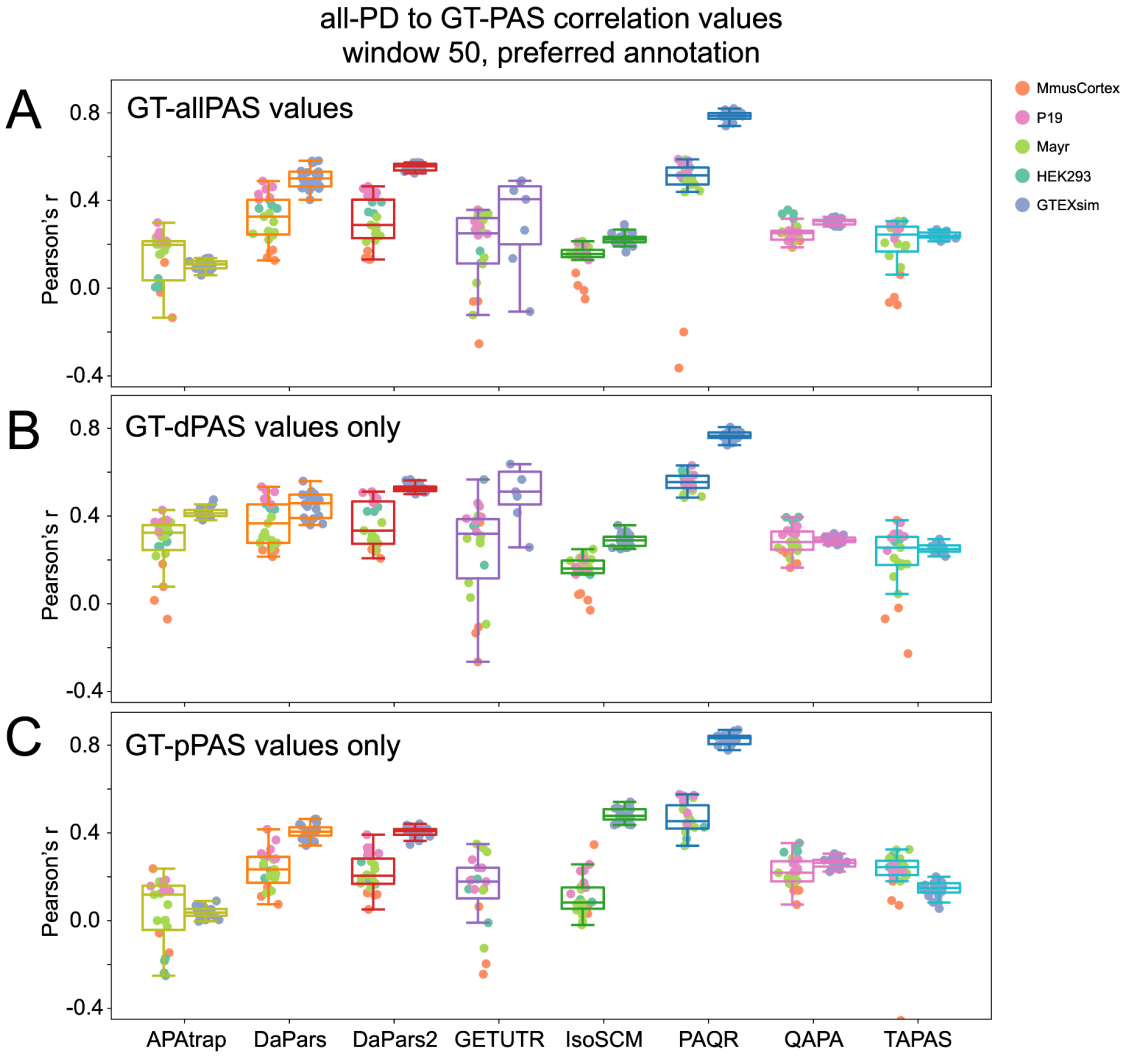

Supplemental Figure 11: The effect of GT-PAS type choice on correlation with predictions (all-PD, preferred annotation): (A) Repeat of Figure 5C shown for comparison. Pearson correlation coefficient when considering all-PD predicted values that match GT-allPAS values (both distal and proximal) using each algorithm's preferred annotation and a match window of 50 nt. Left boxes for each algorithm represent real RNA-seq data and right boxes are simulated RNA-seq data. Each point is labeled according to dataset grouping given in the legend. (B) As in (A), but using all-PD PAS matches to distal GT-PAS (GT-dPAS) values only. (C) As in (A), but using all-PD PAS matches to proximal GT-PAS (GT-pPAS) values only.

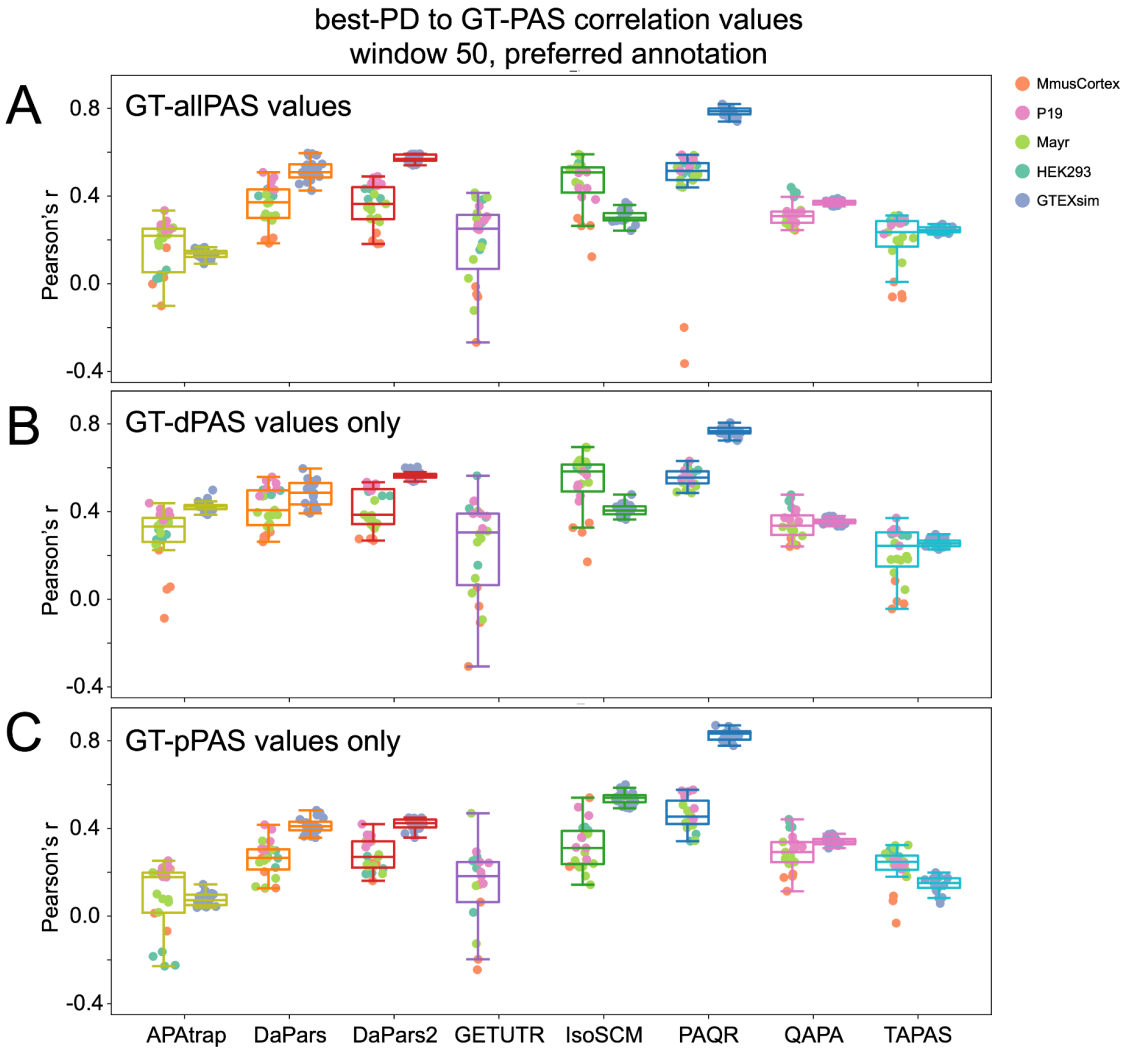

Supplemental Figure 12: The effect of GT-PAS type choice on correlation with predictions (best-PD, preferred annotation): (A) Pearson correlation coefficient when considering the single best-PD predicted values that match GT-allPAS values (both distal and proximal) using each algorithm's preferred annotation and a match window of 50 nt. Left boxes for each algorithm represent real RNA-seq data and right boxes are simulated RNA-seq data. Each point is labeled according to dataset grouping given in the legend. (B) As in (A), but using best-PD PAS matches to distal GT-PAS (GT-dPAS) values only. (C) As in (A), but using best-PD PAS matches to proximal GT-PAS (GT-pPAS) values only.

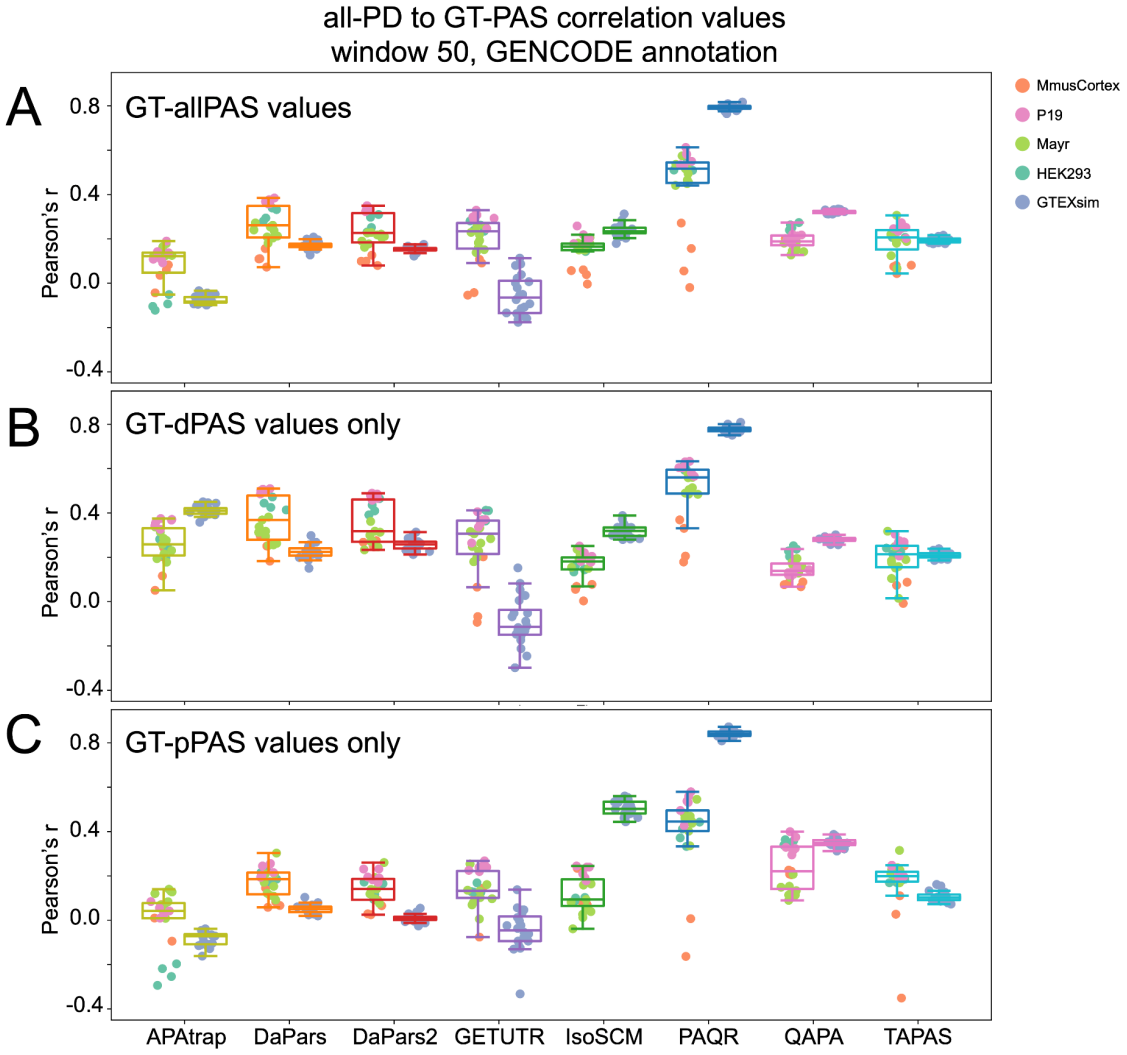

Supplemental Figure 13: The effect of GT-PAS type choice on correlation with predictions (all-PD, GENCODE): (A) Pearson correlation coefficient when considering all-PD predicted values that match GT-allPAS values (both distal and proximal) using GENCODE annotation and a match window of 50 nt. Left boxes for each algorithm represent real RNA-seq data and right boxes are simulated RNA-seq data. Each point is labeled according to dataset grouping given in the legend. (B) As in (A), but using all-PD PAS matches to distal GT-PAS (GT-dPAS) values only. (C) As in (A), but using all-PD PAS matches to proximal GT-PAS (GT-pPAS) values only.

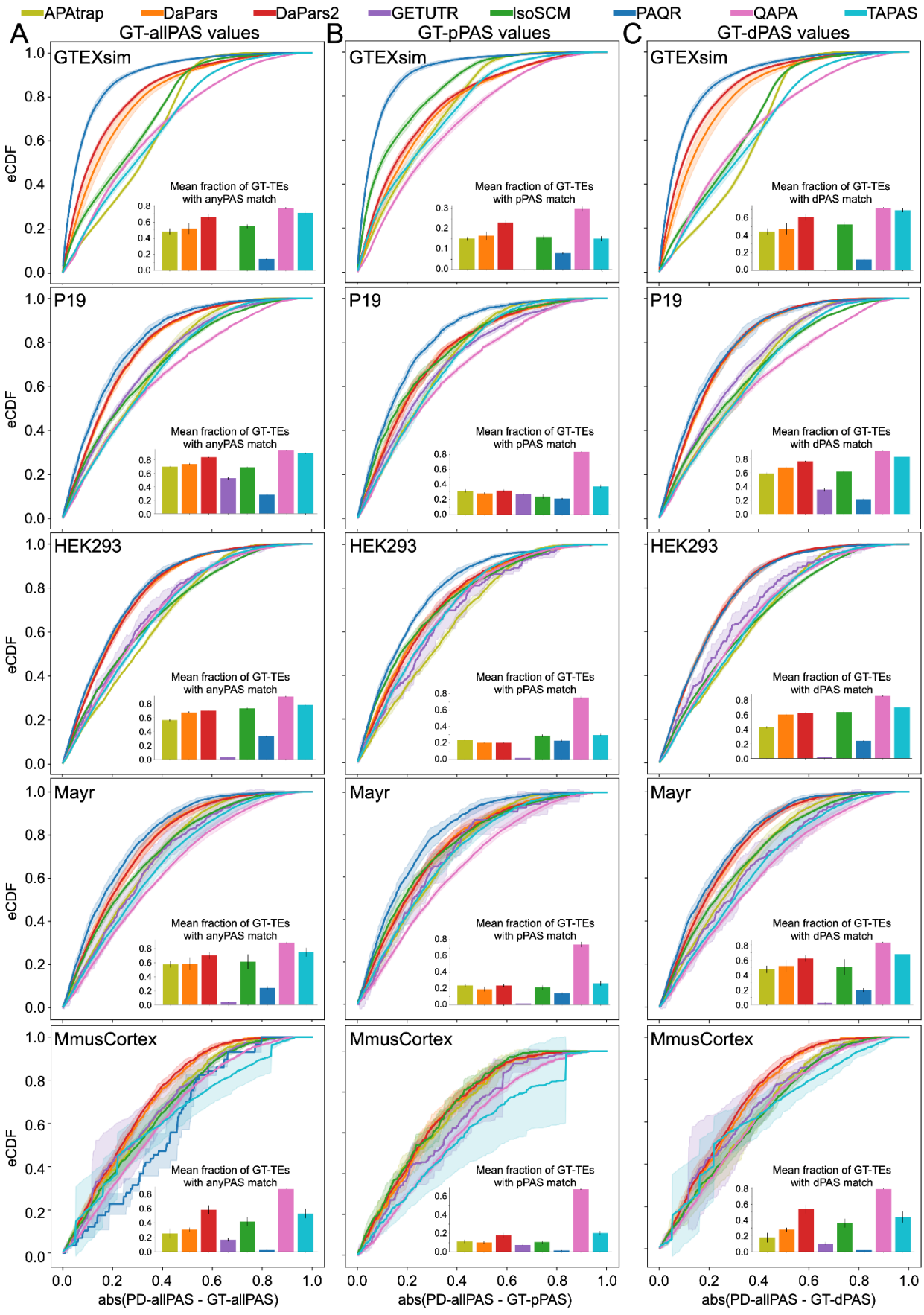
APAtrap
DaPars
DaPars2
GETUTR
IsoSCM
PAQR
QAPA
TAPAS
A
GT-allPAS values
B
GT-pPAS values
C
GT-dPAS values
GTEXsim
P19
HEK293
Mayr
MmusCortex
eCDF
Mean fraction of GT-TEs with anyPAS match
Mean fraction of GT-TEs with pPAS match
Mean fraction of GT-TEs with dPAS match
abs(PD-allPAS - GT-allPAS)
abs(PD-allPAS - GT-pPAS)
abs(PD-allPAS - GT-dPAS)

Supplemental Figure 14. Distribution of absolute differences between ground truth and all prediction values using preferred annotations for all datasets. (A) Average eCDF for the absolute difference between all-PD matches to GT-allPAS values for each algorithm's preferred annotation for the given datasets. Lines represent the mean of all experiments in the group and shaded regions represent plus/minus one SD. Inset barchart shows the mean fraction of unique, ground-truth terminal exons with APA (defined in Figure 4, based on RefSeq annotation) represented by all-PD matches. Error bar shows one SD. Each dataset needed a minimum of 20 matched values to be plotted. (B) Same as (A), but only for matches to proximal GT-PAS (GT-pPAS) values. Inset barchart shows mean fraction of unique GT terminal exons with a pPAS matched to the algorithm predictions. Error bar shows one SD. (C) Same as (A), but only for matches to distal GT-PAS (GT-dPAS) values. Inset barchart shows mean fraction of unique GT terminal exons with a dPAS matched to the algorithm. Error bar shows one SD.

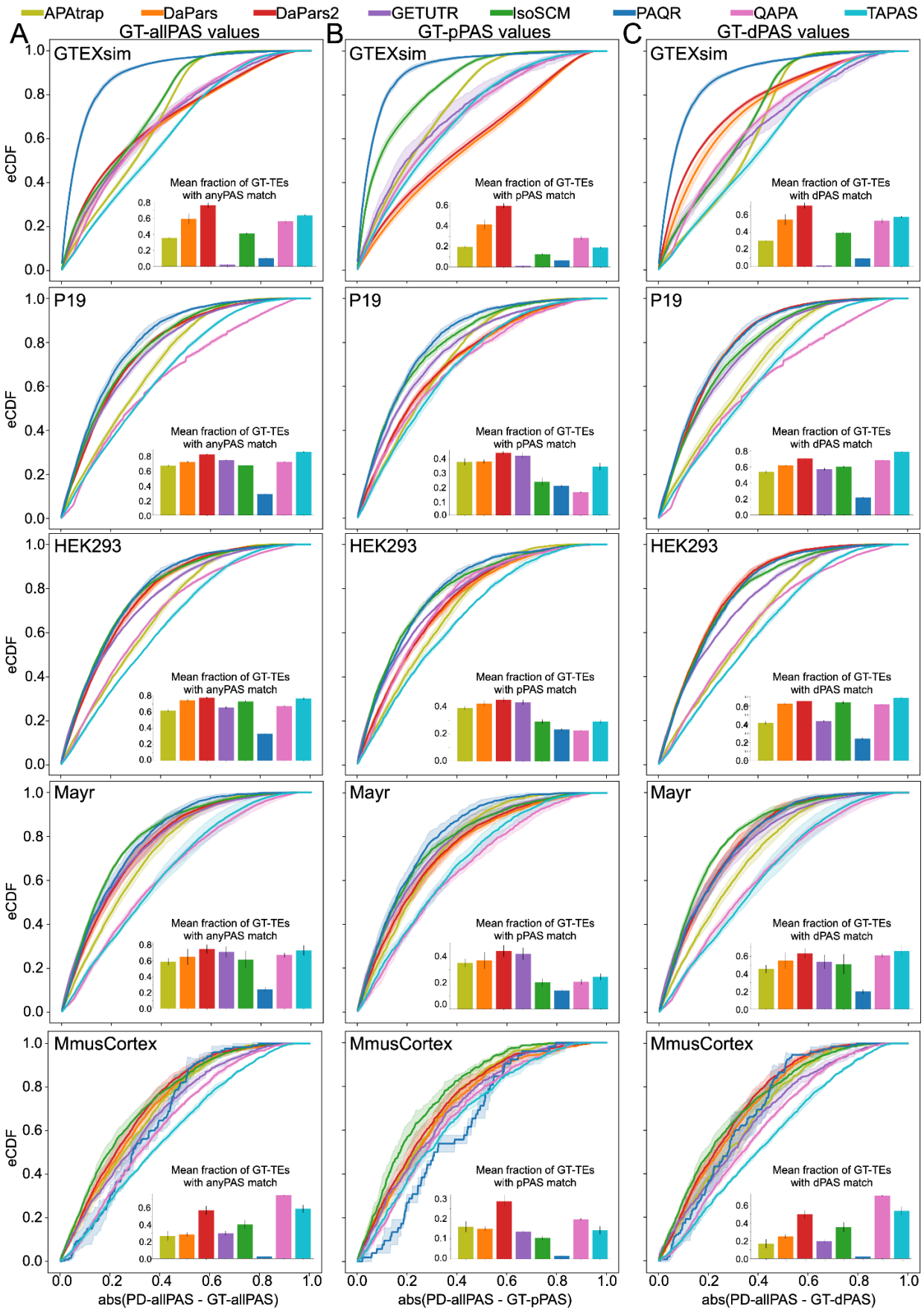
APAtrap
DaPars
DaPars2
GETUTR
IsoSCM
PAQR
QAPA
TAPAS
A
GT-allPAS values
B
GT-pPAS values
C
GT-dPAS values
GTEXsim
P19
HEK293
Mayr
MmusCortex
eCDF
Mean fraction of GT-TEs with anyPAS match
Mean fraction of GT-TEs with pPAS match
Mean fraction of GT-TEs with dPAS match
abs(PD-allPAS - GT-allPAS)
abs(PD-allPAS - GT-pPAS)
abs(PD-allPAS - GT-dPAS)

Supplemental Figure 15. Distribution of absolute differences between ground truth and all prediction values using GENCODE annotations for all datasets. (A) Average eCDF for the absolute difference between all-PD matches to GT-allPAS values for each algorithm using GENCODE annotation for the given datasets. Lines represent the mean of all experiments in the group and shaded regions represent plus/minus one SD. Inset barchart shows the mean fraction of unique, ground-truth terminal exons with APA (defined in Figure 4, based on GENCODE annotation) represented by all-PD matches. Error bar shows one SD. Each dataset needed a minimum of 20 matched values to be plotted. (B) Same as (A), but only for matches to proximal GT-PAS (GT-pPAS) values. Inset barchart shows mean fraction of unique GT terminal exons with a pPAS matched to the algorithm predictions. Error bar shows one SD. (C) Same as (A), but only for matches to distal GT-PAS (GT-dPAS) values. Inset barchart shows mean fraction of unique GT terminal exons with a dPAS matched to the algorithm. Error bar shows one SD.